On the Scalability of Parking Trajectory Optimization of Autonomous Ground Vehicles

Esther Aboyeji
Department of Artificial Intelligence
Kyungpook National University, Daegu,
South Korea.
aboyejitolulopeesther@gmail.com

Oladayo S. Ajani
Department of Artificial Intelligence
Kyungpook National University,
Daegu, South Korea.
oladayosolomon@gmail.com

Rammohan Mallipeddi
Department of Artificial Intelligence
Kyungpook National University
Daegu, South Korea.
mallipeddi.ram@gmail.com

***Abstract*—Although the use of optimization-based algorithms for autonomous motion planning in the context of parking has been studied in the literature, most of the existing works were based on either unrealistic simulation environments or a single vehicle type or model. In order to support the deployment of such frameworks for real-world applications, the need for the scalability analysis of such optimization frameworks under realistic simulation environments as well as different vehicle types becomes important. Therefore this paper investigates the suitability of a two-stage optimization framework under a realistic simulation environment as well as using 4 different vehicle models. Specifically, the two-stage optimization process involves first the use of the A star algorithm for initial path generation, and in the second stage, Sequential Quadratic Programming (SQP) is used to optimize the results pathways. In terms of vehicle type, we employ four different vehicle types with different model parameters and evaluated the performance of the framework accordingly. The results show that also the optimization framework is capable of generating feasible parking trajectories, some vehicle types require more script run-time compared to others.**

***Index Terms*—Autonomous Driving, Trajectory Optimization, Parking Navigation and Maneuvers.**

I. Introduction

Statistics from the 2021 Market Analysis [1], shows that the 51.6 thousand units demanded by the global autonomous vehicle market is expected to increase at a compound annual growth rate (CAGR) of 53.6% from 2022 to 2030. Autonomous Vehicles (AVs) among several other merits are expected to increase road safety, facilitate the reduction of traffic congestion, minimize commute time and harmonize network flow [2]–[4]. Similar to several engineering tasks [5], [6] where different modules are required to complete a task, an AV is enabled by an autonomous driving system which constitutes four major modules namely; Scene Understanding; Localization and Mapping; Planning and Decision; and the Control Module which is responsible for generating appropriate driving actions [7]. From a control perspective, the movement stability of AVs relies on excellent and well-crafted trajectories designed by the motion planning module. As a result, researchers have investigated different trajectory planning schemes for different mission profiles [8]–[12]. In the literature, the use of geometric planners for feasible path generation in order to accomplish pre-planned missions is the most widely studied [13], [14]. However, the use of such geometric planning methods are limited in constrained planning spaces [10].

An example of a constrained planning space is the autonomous parking mission [15], [16] which requires the generation of feasible paths through which a vehicle can navigate and/or maneuver from an origin to a designated location (parking space) depending on the designated performance indices and constraints [13], [14]. In general, autonomous parking is a system of vehicle navigation and maneuvers from a starting point into a parallel, perpendicular, or angled parking slot without manual assistance or operation [17], [18]. Generally, a complete autonomous parking mission includes both navigation and maneuvering. During navigation, the vehicle changes the steering frequently [19] and moves through the regions of the parking space while during maneuvering, the vehicle changes the steering steadily [19] and moves into the parking space. Therefore most studies have considered them separately and designed dedicated algorithms for each task because each task features different performance measures as well as constraints.

Recently, the use of optimization-based algorithms for AV parking has gained a lot of attention [10], [17], [18]. This is because they allow the autonomous parking problem to be formulated and solved as a time-discrete problem. In terms of optimization, both gradient-based and intelligent-based optimization methods have been employed singly or in a combined fashion. Usually, one important goal of such methods is to solve the planning problem in the shortest possible time in terms of script run-time. Among the different works in literature, the scripts run time reported in [20] is within acceptable margins for real-world deployment. However, most of the methods investigated in the literature are based on unrealistic parking space dimensions which leads to unrealistic simulation environments [10], [17], [21] and eventually unrealistic vehicle dimensions. For instance, [22] reports that the standard dimension of a parking space is expected to be within 2.3 to 2.7 m in width and about 3.0 to 6.1 m in length. However, some of the previous works do not consider those dimensions. Similarly, the vehicle dimensions used for experiments in some studies [10], [23], [24] differ from those of a standard vehicle which is expected to be around 4.4 m in length, 1.8 m in width, and 1.5 m in height

[20], [25]. Hence the suitability of the resulting models cannot be guaranteed for real-world implementation. Furthermore, the scalability of the models to different vehicle sizes has not been investigated as most of the works in the literature have only employed a single vehicle type [10], [23], [24]. Although the realistic framework presented in [20] allows comparison with different vehicles; only one vehicle type was used to present the analysis and comparison among several algorithms in which (SQP) performed best.

Therefore in this work, based on the framework proposed in [20], we present a scalability analysis of two-stage optimization-based autonomous vehicle parking missions. In the first stage of the optimization, A star algorithm is used for initial path generation, while in the second stage, SQP is used to optimize the paths. The analysis presented in this work is based on four vehicle names; Land Rover, Seat Ibiza, Seat Leon, and Smart4Two. The four vehicles were chosen because of their different dimensions or sizes and therefore suitable to investigate the different challenges that would be posed to the optimization framework due to the different vehicle dimensions. The results from the analysis based on 24 different parking missions show that although the optimization framework is scalable to the different cars in terms of satisfying all the mission constraints and avoiding collisions, some vehicle types require more script run-time for specific parking missions than others.

The rest of this paper is organized as follows: Section II gives the problem formulation of the parking trajectory optimization problem. Section III shows the framework employed and Section IV presents the experimental results, while the conclusion and future works were given in Section V.

II. Problem Formulation

In this Section, in order to describe the Optimal Control Problem (OCP) for the underlying parking motion planning, mathematical equations, and algebraic equalities/inequalities formulated to aid the description of vehicle dynamics, cost function, and associated constraints are presented. In addition, in the context of optimization, the discretized form of the OCP is detailed.

A. Optimal Control Problem for Parking Motion Planning

A detailed background on a typical OCP can be found in [20] where the dynamics of the system are defined with respect to the dynamics of the underlying vehicle.

1) Model of Vehicle: The schematic diagram of a car-like model as shown in Fig. 1 can be used to describe the motion of the vehicles used in this work. The coordinate of the rear wheel central point of the vehicle is denoted by point (*x, y*), while the inter-axis distance, the rear overhang, the front overhang, the velocity, the acceleration, the angular velocity and the steering angle are denoted by *d, r, f, v, a,* ψ*, and* δ respectively. In order to describe the motion of the vehicle, a 6-dimensional vector denoted by $\dot{q}$ which represents the state of the vehicle is expressed in a system of differential equations as shown in (1). The relationship between the other two vehicle-dependent parameters, i.e. the turn radius ρ and the length between the front and the rear wheel (inter-axis distance) can be expressed mathematically as shown in (2).

$$\dot{q} = \begin{bmatrix} \dot{x} \\ \dot{y} \\ \dot{\psi} \\ \dot{v} \\ \dot{\delta} \\ \dot{a} \end{bmatrix} = f(q,u) = \begin{bmatrix} v\,cos(\psi) \\ v\,sin(\psi) \\ \frac{v}{L}\,tan(\delta) \\ a \\ \frac{\delta_{ref}-\delta}{t_d} \\ \frac{a_{ref}-a}{t_a} \end{bmatrix} \tag{1}$$

$$\rho = \frac{d}{tan(\delta)} \tag{2}$$

The reference steering angle δ_{ref} and the reference longitudinal acceleration a_{ref} are the components of the actual control input u as expressed in equation (1). This 2-dimensional input vector is bounded in a set with upper limits $\delta_{ref,max}$ and $a_{ref,max}$ and lower limits $\delta_{ref,min}$ and $a_{ref,min}$ which can be expressed as follows:

$$u = \begin{bmatrix} \delta_{ref} \\ a_{ref} \end{bmatrix}, \quad \begin{bmatrix} \delta_{ref,min} \\ a_{ref,min} \end{bmatrix} \leq u \leq \begin{bmatrix} \delta_{ref,max} \\ a_{ref,max} \end{bmatrix} \tag{3}$$

It is worth noting that for the purpose of this work, the sideslip of the vehicle model is ignored, however, the dynamics of the actuators are considered as first-order transfer functions with time constraints t_d and t_a.

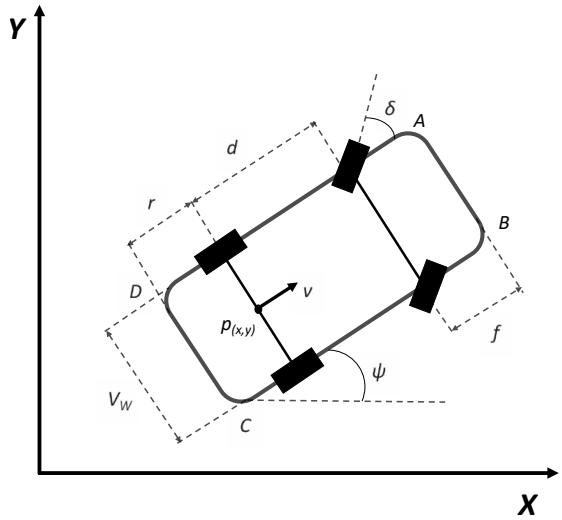

Fig. 1: Schematic representation of a front steering car.

2) Cost Function: In order to solve the OCP problem, the objective or goal of the optimization needs to be defined. In the context of this work, the control objective or goal is to steer the vehicle towards a desired reference state or location (q_{ref}). In other words, the control objective can be expressed in terms of only the terminal state of the motion or vehicle as follows:

$$h(q(T;\,t_0, q_0, u(\cdot))) = \|q_{ref} - q(T;\,t_0, q_0, u(\cdot))\|_W \tag{4}$$

where the initial starting time t_0 and state q_0 are presented under a measurable control $u(\cdot)$. As seen in equation (4), the cost function is expected to be convex with respect to $q(T)$, however, the cost function is non-linear and non-convex because q is mapped to u by a non-linear model with respect to the minimization variable (control history $u(t)$).

3) Parking Constraints: In autonomous parking missions, certain constraints need to be satisfied relative to the underlying parking mission and vehicle model. In reference to [20], Collision Avoidance, Safety and Comfort, and Performance are the constraints featured in this work. Generally, these constraints can be expressed by algebraic equalities/inequalities. Accordingly, the collision constraints are expressed as

$$J_{col}(q(t)) = 0 \tag{5}$$

safety and comfort-related constraints are expressed as:

$$\begin{aligned} -5.0 \leq v(t) \leq 5.0 \quad \forall\, t \in [0,T] \\ -1.0 \leq a_{long}(t) = a(t) \leq 1.0 \quad \forall\, t \in [0,T] \\ -0.8 \leq a_{lat}(t) = \frac{v(t)^2}{\frac{L}{tan(\delta(t))}} \leq 0.8 \quad \forall\, t \in [0,T] \\ -0.7 \leq j_{long}(t) = \frac{a_{ref}(t) - a(t)}{t_a} \leq 0.7 \quad \forall\, t \in [0,T] \\ -0.3 \leq j_{lat}(t) = a_{l\dot{a}t}(t) \leq 0.3 \quad \forall\, t \in [0,T] \end{aligned} \tag{6}$$

where the longitudinal acceleration, the lateral acceleration, the longitudinal jerk, and the lateral jerk are denoted by a_{long}, a_{lat}, j_{long}, and j_{lat} respectively. Lastly, the performance criteria to be satisfied can be formulated as follows:

$$\begin{aligned} \|x_{ref} - x(T)\| \leq 0.1 \\ \|y_{ref} - y(T)\| \leq 0.1 \\ \|\psi_{ref} - \psi(T)\| \leq 0.1 \\ \|v_{ref} - v(T)\| \leq 0.1 \\ \|a_{ref} - a(T)\| \leq 0.1 \end{aligned} \tag{7}$$

where $x_{ref}, y_{ref}, \psi_{ref}, v_{ref}$ and a_{ref} are the parameters that represent the states of the reference state vector q_{ref}.

The overall optimization problem based on the aforementioned cost function and constraints can be summarized as:

$$\begin{aligned} \text{minimize} \quad & J = h(q(T;\, t_0, q_0, u(\cdot))) \\ \text{subject to} \quad & \forall h(q) \in [t_0, q_0, T], \\ & \text{Eq. (5) (Constraints associated with collision),} \\ & \text{Eq. (6) (Safety and Comfort related constraints),} \\ & \text{Eq. (7) (Performance related constraints)} \end{aligned} \tag{8}$$

B. Discritization of the Optimal parking model

It is important to express that the overall optimization problem as presented in (8) is unsolvable in its current state. In order words, the vehicle model, objective function, and constraints need to be discretized and parameterized with respect to time [10], [23]. Generally, this can be achieved by dividing the time interval $[t_0, T]$ into N_k segments, consequently, the optimization problem is equivalent to finding the optimal control values for all the discrete-time instances aimed at minimizing the final state error as well as satisfy the associated constraints. Furthermore, the computation of the state is possible through numerical integration of the dynamics of the system. Accordingly, the optimization problem is re-expressed as:

$$\begin{aligned} \text{minimize} \quad & J = h(q_{N_k}(T_{N_k};\, t_{N_k}, q_{N_k}, u(\cdot))) \\ \text{subject to} \quad & \forall h(q_k), k \in 0, 1, 2, ..., N_k - 1, \\ & \text{Eq. (5) (Constraints associated with collision),} \\ & \text{Eq. (6) (Safety and Comfort related constraints),} \\ & \text{Eq. (7) (Performance related constraints)} \end{aligned} \tag{9}$$

where the equations (5), (6) and (7) are also re-expressed in terms of N_K accordingly [20].

III. Optimization Framework

The optimization framework adopted to solve the OCP and consequently investigate the challenges posed by the use of different vehicle types is detailed in this Section. As mentioned previously, the optimization involves two stages. In the first stage, A star algorithm is used to generate initial waypoints from starting point to the terminal location which is the parking lot. Specifically, the A star algorithm is used to generate these waypoints for both the navigation and maneuvering process of the parking mission. Consequently, these resulting waypoints are reduced or broken into segments where each segment can be solved in the second stage as a local planning problem. In order to proceed with the second stage of the optimization, the planning horizon needs to be set. The planning horizon generally is the number of waypoints assigned into each segments of the local planning problem. The objective of the local planing problem to be solved in the second stage is formulated such that the start or initial point is taken as the final states of earlier segments and the terminal point is taken as the last waypoint in the current segment. The approach mimics how humans solves a typical parking problem where although the ultimate goal is the parking spot, the motion is planned and execute step by step until the final goal is achieved.

Considering that the second stage is a local search problem, gradient-based optimization algorithms are often employed. Among different gradient-based algorithms such as Interior-point method (IPM), SQP, Trust region, and Active-set evaluated in [20], SQP demonstrated a superior performance in all the metrics compared to the other algorithms. Therefore we use SQP for the optimization in the second stage.

IV. Experimental Setup and Results

In this Section, the protocols and results of the experiments conducted to investigate the scalability of a two-stage optimization-based autonomous parking framework are

presented. Specifically, the experiments are conducted with four different vehicle types on 24 different parking missions.

A. Experimental Setup and Metrics

Figure 2 shows the layout of the 24 different parking missions employed in this work. In the figure, each number represents different parking spaces corresponding to each of the parking missions. In Table, I, the parameters of the vehicle models used for comparison namely; Land-Rover Defender, SEAT Ibiza, SEAT Leon, and Smart4Two in terms of vehicle-related control parameters and vehicle dimension, are presented. Furthermore, in Table II the mission-related parameters such as parking space length (P_{SL}), parking space width (P_{SW}), parking lane width (P_{LW}), as well as the range of mission-related variables are represented in Table I.

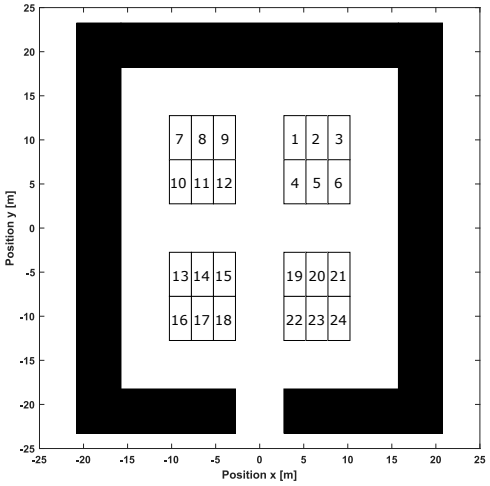

Fig. 2: Parking environment layout and 24 parking missions showing the parking space dimensions of 2.5x5.0 m and lane width of 5.5 m.

TABLE I: Values of Control Parameters

Land-Rover		**Seat_Ibiza**		**Seat_Leon**		**Smart4two**	
Parameters	**Values**	**Parameters**	**Values**	**Parameters**	**Values**	**Parameters**	**Values**
V_L, m	4.639	V_L, m	4.059	V_L, m	4.263	V_L, m	2.695
V_W, m	1.79	V_W, m	1.942	V_W, m	1.975	V_W, m	1.663
d, m	2.794	d, m	2.564	d, m	2.636	d, m	1.873
f, m	0.645	f, m	0.796	f, m	0.842	f, m	0.402
r, m	1.2	r, m	0.699	r, m	0.785	r, m	0.42

TABLE II: Ranges of Variables

Variables	Ranges	Variables	Ranges
P_{SL}, m	5	v, m/s	[-5.0, 5.0]
P_{SW}, m	2.5	a_{long}, m/s^2	[-1.0, 1.0]
P_{LW}, m	5.5	a_{lat}, m/s^2	[-0.8, 0.8]
p_x, m	[-15, 15]	δ, deg	[-37, 37]
p_y, m	[-25, 25]		

Commonly used metrics for performance evaluation optimization-based autonomous parking in the literature includes motion length, objective value, collision rate, and satisfaction of mission performance constraints [23]. In this work, in addition to those metrics, we also employ the script run-time which is a measure of how much time it takes the planner to plan the parking mission. For the sake of vehicle-wise comparison, the mean and standard deviation values of each of the aforementioned metrics obtained over six independent runs of the algorithm using each of the four vehicle types on each of the 24 parking missions are presented. In terms of the collision rate metric, zero (0) implies that no collision occurred while one (1) implies the occurrence of collision. On the contrary, for the Mission Performance Constraints Satisfaction (MPCS), zero (0) implies that all the mission constraints were not satisfied while one (1) means otherwise. Basically, as formulated in [20], the performance constraints are said to be met once the objective function value is equal to or less than 0.1. Finally, all the experiments conducted in this work are carried out in MATLAB installed on 64-bit Windows 10 PC, Intel(R) Core(TM) i9-11900K at 3.50GHZ with 32GB RAM.

B. Experimental Results

Tables III and IV present the simulation results of trajectory planning for 4 different vehicles in terms of the aforementioned metrics. Specifically, Table III presents results in terms of objective value, collision rate, and MPCS while Table IV presents results in terms of script run-time, and motion length respectively. Generally, the optimization framework proves scalable in terms of the objective value and associated constraints across the four vehicle types and all 24 parking missions. As shown in Table III, all the objective values are within the allowable limits, and all the performance-related constraints are satisfied without collision.

The mean and standard deviation of run-time for all four vehicle types on the 24 different parking missions reported in Table IV are comparable except for three parking missions (16, 17, and 18) where the script run-time for Seat Leon was relatively higher compared to the other vehicles as clearly shown in 3 which present heatmap showing the run-time for all the vehicles across the 24 mission cases. In terms of the average motion length, although it is clear from 4 which presents a heatmap showing the motion length for all the vehicles across the 24 mission cases that the average motion lengths are comparable, some parking missions have a higher motion length across all the vehicles compared to others. This is expected because the distance from the start point to the parking spot for all 24 parking missions is not the same. Furthermore, it can be observed generally that the Smart4Two vehicle as a lower motion length compared to all the other vehicles in all instances of the 24 parking mission.

V. Conclusion and Future Works

This paper demonstrates the scalability of a two-stage optimization framework for parking trajectory optimization of 4 different autonomous ground vehicles over 24 different parking missions. In the first stage of the optimization, A star algorithm is used to generate initial waypoints for both the navigation and maneuvering process of the parking mission. Consequently, these resulting waypoints are reduced or broken into segments where each segment can be solved in the second stage as a local planning problem. To solve the resulting local

TABLE III: Performance of different vehicle types on 24 parking missions based on objective value, average collisions and average mission performance criteria satisfaction.

Case	Land Rover				Seat Ibiza				Seat Leon				Smart4two			
	Obj Value		Collision	MPCS	Obj Value		Collision	MPCS	Obj Value		Collision	MPCS	Obj Value		Collision	MPCS
	Mean	Std Dev			Mean	Std Dev			Mean	Std Dev			Mean	Std Dev		
1	8.41E-03	1.73E-18	0	1 ± 0	5.71E-03	9.50E-19	0	1 ± 0	7.91E-03	1.73E-18	0	1 ± 0	7.00E-03	0.00E+00	0	1 ± 0
2	9.08E-03	1.73E-18	0	1 ± 0	5.92E-03	0.00E+00	0	1 ± 0	6.93E-03	8.67E-19	0	1 ± 0	6.43E-03	8.67E-19	0	1 ± 0
3	5.09E-03	0.00E+00	0	1 ± 0	4.75E-03	0.00E+00	0	1 ± 0	5.86E-03	0.00E+00	0	1 ± 0	7.67E-03	8.67E-19	0	1 ± 0
4	9.72E-03	0.00E+00	0	1 ± 0	4.18E-03	9.50E-19	0	1 ± 0	6.59E-03	8.67E-19	0	1 ± 0	6.78E-03	0.00E+00	0	1 ± 0
5	8.01E-03	1.73E-18	0	1 ± 0	9.85E-03	0.00E+00	0	1 ± 0	9.38E-03	0.00E+00	0	1 ± 0	5.37E-03	0.00E+00	0	1 ± 0
6	8.79E-03	0.00E+00	0	1 ± 0	6.07E-03	0.00E+00	0	1 ± 0	8.69E-03	0.00E+00	0	1 ± 0	9.87E-03	0.00E+00	0	1 ± 0
7	8.69E-03	1.73E-18	0	1 ± 0	7.89E-03	1.90E-18	0	1 ± 0	5.84E-03	0.00E+00	0	1 ± 0	9.40E-03	0.00E+00	0	1 ± 0
8	7.31E-03	0.00E+00	0	1 ± 0	7.04E-03	0.00E+00	0	1 ± 0	9.63E-03	0.00E+00	0	1 ± 0	7.88E-03	0.00E+00	0	1 ± 0
9	6.32E-03	8.67E-19	0	1 ± 0	9.91E-03	0.00E+00	0	1 ± 0	7.08E-03	8.67E-19	0	1 ± 0	9.75E-03	0.00E+00	0	1 ± 0
10	7.67E-03	0.00E+00	0	1 ± 0	5.90E-03	0.00E+00	0	1 ± 0	4.76E-03	0.00E+00	0	1 ± 0	9.50E-03	0.00E+00	0	1 ± 0
11	7.03E-03	0.00E+00	0	1 ± 0	8.69E-03	0.00E+00	0	1 ± 0	9.96E-03	0.00E+00	0	1 ± 0	9.94E-03	1.73E-18	0	1 ± 0
12	7.37E-03	8.67E-19	0	1 ± 0	2.92E-03	0.00E+00	0	1 ± 0	9.82E-03	0.00E+00	0	1 ± 0	8.60E-03	0.00E+00	0	1 ± 0
13	8.41E-03	1.73E-18	0	1 ± 0	6.61E-03	0.00E+00	0	1 ± 0	3.56E-03	0.00E+00	0	1 ± 0	9.49E-03	0.00E+00	0	1 ± 0
14	8.97E-03	1.73E-18	0	1 ± 0	6.56E-03	9.50E-19	0	1 ± 0	7.35E-03	0.00E+00	0	1 ± 0	8.85E-03	0.00E+00	0	1 ± 0
15	9.88E-03	1.73E-18	0	1 ± 0	9.59E-03	0.00E+00	0	1 ± 0	7.27E-03	0.00E+00	0	1 ± 0	9.47E-03	1.73E-18	0	1 ± 0
16	8.26E-03	0.00E+00	0	1 ± 0	5.32E-03	0.00E+00	0	1 ± 0	5.83E-03	8.67E-19	0	1 ± 0	8.06E-03	0.00E+00	0	1 ± 0
17	6.73E-03	0.00E+00	0	1 ± 0	9.59E-03	0.00E+00	0	1 ± 0	9.72E-03	0.00E+00	0	1 ± 0	8.57E-03	1.73E-18	0	1 ± 0
18	2.29E-03	0.00E+00	0	1 ± 0	9.28E-03	1.90E-18	0	1 ± 0	6.79E-03	0.00E+00	0	1 ± 0	9.09E-03	0.00E+00	0	1 ± 0
19	9.57E-03	0.00E+00	0	1 ± 0	5.17E-03	9.50E-19	0	1 ± 0	6.83E-03	0.00E+00	0	1 ± 0	7.85E-03	1.73E-18	0	1 ± 0
20	6.88E-03	0.00E+00	0	1 ± 0	9.69E-03	1.90E-18	0	1 ± 0	7.29E-03	0.00E+00	0	1 ± 0	9.49E-03	0.00E+00	0	1 ± 0
21	9.16E-03	1.73E-18	0	1 ± 0	3.17E-03	4.75E-19	0	1 ± 0	5.76E-03	0.00E+00	0	1 ± 0	7.29E-03	0.00E+00	0	1 ± 0
22	6.98E-03	8.67E-19	0	1 ± 0	9.51E-03	0.00E+00	0	1 ± 0	9.88E-03	0.00E+00	0	1 ± 0	8.79E-03	0.00E+00	0	1 ± 0
23	7.94E-03	0.00E+00	0	1 ± 0	8.86E-03	0.00E+00	0	1 ± 0	9.93E-03	0.00E+00	0	1 ± 0	8.65E-03	0.00E+00	0	1 ± 0
24	9.97E-03	0.00E+00	0	1 ± 0	8.76E-03	1.90E-18	0	1 ± 0	5.22E-03	8.67E-19	0	1 ± 0	6.74E-03	0.00E+00	0	1 ± 0

TABLE IV: Performance of different vehicle types on 24 parking missions based on average run time and length of motion.

Case	Land Rover				Seat Ibiza				Seat Leon				Smart4two			
	Run Time		Motion Length		Run Time		Motion Length		Run Time		Motion Length		Run Time		Motion Length	
	Mean	Std Dev	Mean	Std Dev	Mean	Std Dev	Mean	Std Dev	Mean	Std Dev	Mean	Std Dev	Mean	Std Dev	Mean	Std Dev
1	1.91E+00	3.51E-01	5.38E+01	7.11E-15	1.92E+00	4.45E-01	5.35E+01	7.78E-15	1.71E+00	2.75E-01	5.35E+01	0.00E+00	1.79E+00	3.14E-01	4.84E+01	0.00E+00
2	1.57E+00	2.44E-02	5.63E+01	0.00E+00	1.50E+00	2.38E-02	5.60E+01	7.78E-15	1.50E+00	2.44E-02	5.60E+01	0.00E+00	1.39E+00	2.38E-02	5.12E+01	7.11E-15
3	1.67E+00	3.19E-03	5.69E+01	0.00E+00	1.69E+00	1.86E-02	5.65E+01	0.00E+00	1.71E+00	1.86E-02	5.65E+01	7.11E-15	1.37E+00	4.52E-03	5.38E+01	0.00E+00
4	1.37E+00	6.32E-03	3.75E+01	7.11E-15	1.38E+00	1.01E-02	3.75E+01	7.78E-15	1.34E+00	1.08E-02	3.74E+01	7.11E-15	1.26E+00	4.13E-03	3.37E+01	7.11E-15
5	1.44E+00	2.14E-02	4.01E+01	0.00E+00	1.38E+00	1.03E-02	4.00E+01	0.00E+00	1.36E+00	9.22E-03	4.00E+01	0.00E+00	1.31E+00	3.33E-02	3.61E+01	0.00E+00
6	1.41E+00	1.69E-02	4.06E+01	0.00E+00	1.45E+00	8.72E-03	4.05E+01	7.78E-15	1.36E+00	8.09E-03	4.05E+01	7.11E-15	1.48E+00	2.88E-03	3.85E+01	0.00E+00
7	1.55E+00	1.46E-02	5.59E+01	0.00E+00	1.53E+00	1.72E-02	5.56E+01	0.00E+00	1.66E+00	1.09E-02	5.57E+01	0.00E+00	1.37E+00	4.68E-03	5.33E+01	0.00E+00
8	1.53E+00	4.47E-03	5.54E+01	7.11E-15	1.47E+00	2.72E-02	5.51E+01	0.00E+00	1.49E+00	1.96E-02	5.52E+01	0.00E+00	1.53E+00	3.77E-02	5.08E+01	0.00E+00
9	1.55E+00	2.89E-02	5.29E+01	0.00E+00	1.46E+00	9.49E-03	5.26E+01	0.00E+00	1.49E+00	1.63E-02	5.29E+01	0.00E+00	1.52E+00	1.81E-02	4.79E+01	0.00E+00
10	1.37E+00	2.19E-02	4.01E+01	0.00E+00	1.35E+00	2.23E-02	3.97E+01	0.00E+00	1.35E+00	2.25E-02	3.99E+01	0.00E+00	1.32E+00	2.64E-02	3.78E+01	0.00E+00
11	1.36E+00	6.83E-03	3.96E+01	7.11E-15	1.33E+00	5.40E-03	3.91E+01	7.78E-15	1.36E+00	6.36E-03	3.93E+01	0.00E+00	1.40E+00	1.10E-02	3.53E+01	0.00E+00
12	1.37E+00	1.53E-02	3.71E+01	0.00E+00	1.34E+00	4.61E-03	3.66E+01	7.78E-15	1.32E+00	1.28E-02	3.68E+01	0.00E+00	1.39E+00	2.50E-02	3.31E+01	0.00E+00
13	1.39E+00	1.94E-03	4.02E+01	0.00E+00	3.97E+01	7.78E-15	3.97E+01	7.78E-15	1.34E+00	3.63E-03	3.99E+01	0.00E+00	1.34E+00	9.97E-03	3.78E+01	0.00E+00
14	1.37E+00	1.37E-02	3.96E+01	0.00E+00	1.33E+00	4.22E-03	3.92E+01	0.00E+00	1.37E+00	1.16E-02	3.94E+01	0.00E+00	1.43E+00	3.89E-03	3.52E+01	7.11E-15
15	1.33E+00	7.39E-03	3.72E+01	7.11E-15	1.36E+00	1.54E-02	3.67E+01	0.00E+00	1.35E+00	2.41E-02	3.69E+01	0.00E+00	1.34E+00	2.39E-03	3.21E+01	7.11E-15
16	1.28E+00	6.61E-03	2.48E+01	3.55E-15	1.29E+00	3.24E-03	2.42E+01	0.00E+00	3.12E+00	4.72E-02	2.52E+01	0.00E+00	1.29E+00	4.42E-03	2.25E+01	0.00E+00
17	1.31E+00	5.16E-03	2.42E+01	0.00E+00	1.25E+00	5.80E-03	2.37E+01	0.00E+00	3.01E+00	7.05E-03	2.46E+01	0.00E+00	1.34E+00	3.22E-03	2.00E+01	0.00E+00
18	1.22E+00	3.39E-03	2.16E+01	0.00E+00	1.25E+00	4.21E-03	2.11E+01	0.00E+00	3.00E+00	8.32E-03	2.21E+01	3.55E-15	1.22E+00	2.18E-03	1.77E+01	0.00E+00
19	1.36E+00	2.55E-03	3.78E+01	7.11E-15	1.35E+00	7.38E-03	3.77E+01	0.00E+00	1.32E+00	2.44E-03	3.78E+01	0.00E+00	1.31E+00	6.06E-03	3.26E+01	0.00E+00
20	1.36E+00	3.82E-03	4.03E+01	0.00E+00	1.38E+00	3.94E-03	4.02E+01	0.00E+00	1.38E+00	5.16E-03	4.03E+01	0.00E+00	1.38E+00	5.78E-03	3.56E+01	7.11E-15
21	1.39E+00	7.79E-03	4.09E+01	7.11E-15	1.38E+00	1.07E-02	4.08E+01	0.00E+00	1.38E+00	1.24E-02	4.08E+01	7.11E-15	1.53E+00	1.15E-02	3.81E+01	7.11E-15
22	1.26E+00	3.48E-03	2.21E+01	0.00E+00	1.23E+00	3.68E-03	2.15E+01	0.00E+00	1.24E+00	3.04E-03	2.16E+01	0.00E+00	1.25E+00	8.50E-03	1.81E+01	0.00E+00
23	1.31E+00	2.97E-03	2.46E+01	3.55E-15	1.29E+00	8.69E-03	2.40E+01	0.00E+00	1.29E+00	5.49E-03	2.41E+01	0.00E+00	1.23E+00	4.36E-03	2.06E+01	0.00E+00
24	1.29E+00	1.31E-02	2.51E+01	0.00E+00	1.41E+00	3.07E-03	2.46E+01	3.89E-15	1.25E+00	5.11E-03	2.47E+01	0.00E+00	1.36E+00	3.58E-03	2.27E+01	0.00E+00

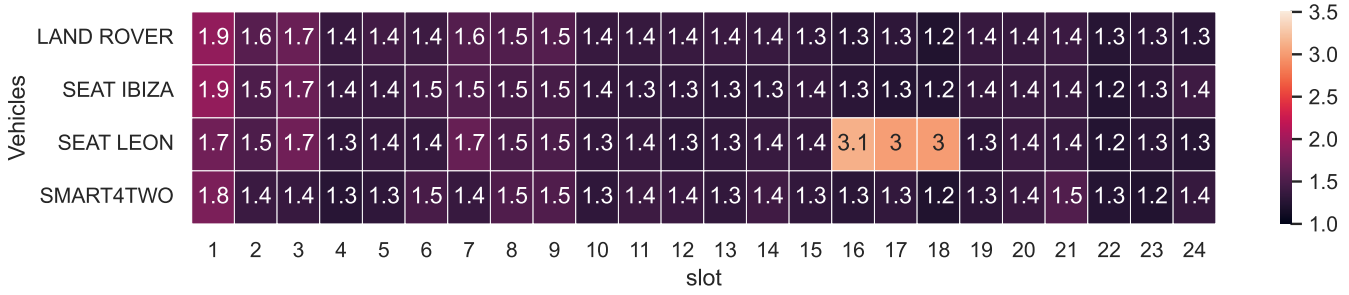

Fig. 3: Heatmap showing the run time for each vehicle across 24 mission cases.

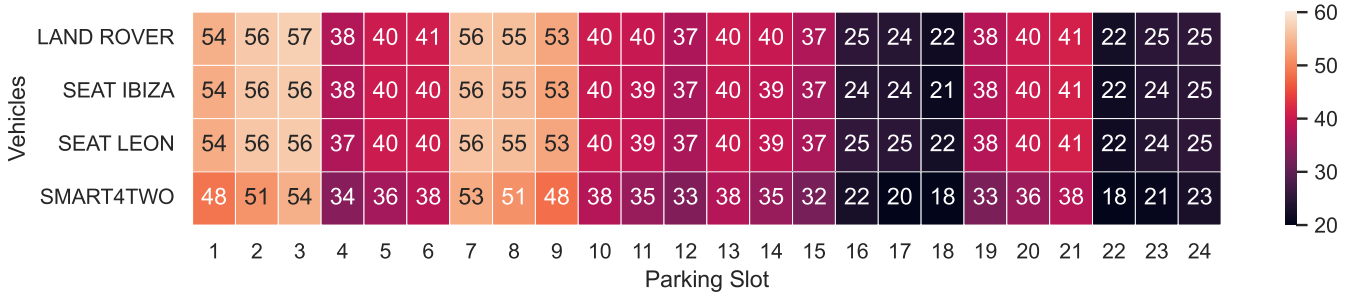

Fig. 4: Heatmap showing the motion length for each vehicle across 24 mission cases.

planning problem from stage one, SQP is employed in the second stage of the optimization. The results show that the optimization framework is scalable to different vehicle types in terms of the objective as well as associated mission constraints.

In the future, we plan to investigate the scalability of the second stage of the optimization to different planning horizons because in the context of control (usually based on model predictive control), long planning horizons are favorable compared to the small planning horizon employed in this study.

Acknowledgement

This research was supported by the Core Research Institute Basic Science Research Program through the National Research Foundation of Korea(NRF) funded by the Ministry of Education (2021R1A6A1A03043144) and the National Research Foundation of Korea (NRF) under project BK21.

References

[1] G. view research, "Autonomous vehicles market size, share, trends analysis report by application (transportation, defense), by region (north america, europe, asia pacific, south america, mea) and segment forecasts, 2022 - 2030," pp. 2022–2030, 2022.

[2] I. Nastjuk, B. Herrenkind, M. Marrone, A. B. Brendel, and L. M. Kolbe, "What drives the acceptance of autonomous driving? an investigation of acceptance factors from an end-user's perspective," *Technological Forecasting and Social Change*, vol. 161, p. 120319, 2020.

[3] M. Ghatee, "Optimization techniques in intelligent transportation systems," *Metaheuristics and Optimization in Computer and Electrical Engineering*, pp. 49–92, 2021.

[4] M. Ghatee and S. M. Hashemi, "Descent direction algorithm with multi-commodity flow problem for signal optimization and traffic assignment jointly," *Appl. Math. Comput.*, vol. 188, no. 1, pp. 555–566, 2007.

[5] A. S. Oladayo, F. M. Samy Assal, and H. El-Hussieny, "Towards development of an autonomous robotic system for beard shaving assistance for disabled people," in *2019 IEEE International Conference on Systems, Man and Cybernetics (SMC)*, 2019, pp. 3435–3440.

[6] O. S. Ajani and S. F. M. Assal, "Hybrid force tracking impedance control-based autonomous robotic system for tooth brushing assistance of disabled people," *IEEE Transactions on Medical Robotics and Bionics*, vol. 2, no. 4, pp. 649–660, 2020.

[7] B. R. Kiran, I. Sobh, V. Talpaert, P. Mannion, A. A. Al Sallab, S. Yogamani, and P. Pérez, "Deep reinforcement learning for autonomous driving: A survey," *IEEE Transactions on Intelligent Transportation Systems*, vol. 23, no. 6, pp. 4909–4926, 2021.

[8] B. Tian, W. Fan, R. Su, and Q. Zong, "Real-time trajectory and attitude coordination control for reusable launch vehicle in reentry phase," *IEEE Transactions on Industrial Electronics*, vol. 62, no. 3, pp. 1639–1650, 2014.

[9] G. Xie, H. Gao, L. Qian, B. Huang, K. Li, and J. Wang, "Vehicle trajectory prediction by integrating physics-and maneuver-based approaches using interactive multiple models," *IEEE Transactions on Industrial Electronics*, vol. 65, no. 7, pp. 5999–6008, 2017.

[10] R. Chai, A. Tsourdos, A. Savvaris, S. Chai, Y. Xia, and C. P. Chen, "Multiobjective overtaking maneuver planning for autonomous ground vehicles," *IEEE Trans Cybern*, vol. 51, no. 8, pp. 4035–4049, 2020.

[11] C. Sun, Y.-C. Liu, R. Dai, and D. Grymin, "Two approaches for path planning of unmanned aerial vehicles with avoidance zones," *Journal of Guidance, Control, and Dynamics*, vol. 40, no. 8, pp. 2076–2083, 2017.

[12] Y. Wang, S. Wang, M. Tan, C. Zhou, and Q. Wei, "Real-time dynamic dubins-helix method for 3-d trajectory smoothing," *IEEE Trans. Control Syst.*, vol. 23, no. 2, pp. 730–736, 2014.

[13] T. Mercy, R. Van Parys, and G. Pipeleers, "Spline-based motion planning for autonomous guided vehicles in a dynamic environment," *IEEE Trans. Control Syst.*, vol. 26, no. 6, pp. 2182–2189, 2017.

[14] F. You, R. Zhang, G. Lie, H. Wang, H. Wen, and J. Xu, "Trajectory planning and tracking control for autonomous lane change maneuver based on the cooperative vehicle infrastructure system," *Expert Systems with Applications*, vol. 42, no. 14, pp. 5932–5946, 2015.

[15] J. Moon, I. Bae, J.-g. Cha, and S. Kim, "A trajectory planning method based on forward path generation and backward tracking algorithm for automatic parking systems," in *17th International IEEE Conference on Intelligent Transportation Systems (ITSC)*. IEEE, 2014, pp. 719–724.

[16] B. Li, K. Wang, and Z. Shao, "Time-optimal maneuver planning in automatic parallel parking using a simultaneous dynamic optimization approach," *IEEE Transactions on Intelligent Transportation Systems*, vol. 17, no. 11, pp. 3263–3274, 2016.

[17] D. M. Filatov, E. V. Serykh, M. M. Kopichev, and A. V. Weinmeister, "Autonomous parking control system of four-wheeled vehicle," in *2016 IEEE V Forum Strategic Partnership of Universities and Enterprises of Hi-Tech Branches (Science. Education. Innovations)*. IEEE, 2016, pp. 102–107.

[18] L. Bai and S. Zhijiang, "Autonomous parking: A unified motion planning framework based on simultaneous dynamic optimization," in *2015 34th Chinese Control Conference (CCC)*. IEEE, 2015, pp. 5913–5918.

[19] J. Leu, Y. Wang, M. Tomizuka, and S. Di Cairano, "Autonomous vehicle parking in dynamic environments: An integrated system with prediction and motion planning," in *2022 International Conference on Robotics and Automation (ICRA)*. IEEE, 2022, pp. 10 890–10 897.

[20] R. Cirera Rocosa, "Motion planning for non-holonomic autonomous vehicles in parking spaces: An optimal control problem approach," 2018.

[21] B. Li and Z. Shao, "Simultaneous dynamic optimization: A trajectory planning method for nonholonomic car-like robots," *Advances in Engineering Software*, vol. 87, pp. 30–42, 2015.

[22] P. Mobilty, "How wide is a parking space?" 2020.

[23] R. Chai, A. Tsourdos, A. Savvaris, S. Chai, and Y. Xia, "Two-stage trajectory optimization for autonomous ground vehicles parking maneuver," *IEEE Transactions on Industrial Informatics*, vol. 15, no. 7, pp. 3899–3909, 2019.

[24] R. Chai, A. Tsourdos, A. Savvaris, S. Chai, Y. Xia, and C. P. Chen, "Multiobjective optimal parking maneuver planning of autonomous wheeled vehicles," *IEEE Transactions on Industrial Electronics*, vol. 67, no. 12, pp. 10 809–10 821, 2020.

[25] NimbleFins, "What are the average dimensions of a car in the UK?" 2021.